ELSEVIER

Journal of Alloys and Compounds 434–435 (2007) 48–51

Journal of ALLOYS AND COMPOUNDS

www.elsevier.com/locate/jallcom

Shear-band propagation in fully amorphous and partially crystallized Mg-based alloys studied by nanoindentation and transmission electron microscopy

A. Castellero [a,b,*], S.J. Lloyd [a], S.V. Madge [a,c], Zs. Kovacs [d], J.F. Löffler [b], M. Baricco [e], A.L. Greer [a]

[a] *Department of Materials Science and Metallurgy, University of Cambridge, Pembroke Street, Cambridge CB2 3QZ, UK*
[b] *Laboratory of Metal Physics and Technology, Department of Materials, ETH Zürich, Wolfgang-Pauli-Strasse 10, CH-8093 Zürich, Switzerland*
[c] *International Advanced Research Centre for Powder Metallurgy & New Materials (ARCI), PO Balapur, Hyderabad 500 005, India*
[d] *Department of General Physics, Eötvös Loránd University, Pázmány P. sétány 1/a, 1117 Budapest, Hungary*
[e] *Dipartimento di Chimica I.F.M. and N.I.S., Università degli Studi di Torino, Via P. Giuria 9, I-10125 Torino, Italy*

Available online 2 October 2006

Abstract

Fully amorphous and partially crystallized $Mg_{66}Ni_{20}Nd_{14}$ and partially crystallized $Mg_{60}Cu_{30}Y_{10}$ alloys were indented and, subsequently, thinned along the cross-section of the indent by means of a focused ion beam (FIB) for transmission electron microscopy (TEM) observation. Depending on the crystallized fraction and the crystal size, the volume deformed under the indenter tip shows different features that can be associated with the different ability of the shear bands to propagate in the two partially devitrified metallic glasses.

Keywords: Metallic glass; Nanoindentation; Shear band; Focused ion beam; TEM

1. Introduction

It is well known that plastic flow in metallic glasses is localized in narrow regions called shear or slip bands, which are characterized by an excess of free volume [1,2]. The first transmission electron microscopy (TEM) observations of shear bands showed thicknesses between 10 and 60 nm, depending on testing conditions [3]. On the basis of the electron diffraction patterns and dark-field images, shear bands seem to contain low-density material due to the presence of voids with a diameter between 0.3 and 0.8 nm [3]. More recently, Li et al. [4] observed, by means of quantitative high-resolution transmission electron microscopy (HRTEM), the presence of nanometer-scale voids within shear bands, which were correlated with the coalescence of excess free volume following plastic flow.

The activity of shear bands can be revealed by instrumented indentation techniques. In the last few years several authors [5–8] reported the presence of constant-load steps in the loading curve, which are related to the serrated plastic flow typical of a metallic glass. A detailed analysis of the pop-in events can be found in Refs. [9,10]. The effect of crystal size on the nanoindentation response and shear-band propagation in a partially crystallized metallic glass is reported in Ref. [7]. The different behaviour of two partially devitrified Fe-based alloys with different crystal sizes can be explained by assuming that only crystals larger than the shear-band thickness are able to deflect or stop their propagation. When the crystal diameter is of the same order of magnitude as the shear-band thickness, their propagation is not affected by the presence of the crystals.

2. Experimental

Amorphous rods of composition $Mg_{60}Cu_{30}Y_{10}$ and $Mg_{66}Ni_{20}Nd_{14}$ (nominal composition, at.%) were prepared by casting in a copper mould. Partial crystallization of the samples was achieved by isothermal annealing. Structural characterization of the samples, both fully amorphous and partially crystallized, was performed by X-ray diffraction (XRD) with Cu Kα radiation. Depth-sensing indentation was carried out using a Nanotest 600 instrument (Micro Materials Ltd., UK) fitted with a Berkovich indenter. Penetration depths were in the range of 0.2–1.8 μm, and the loading and unloading rate ranged from 0.5 to 10.0 mN s^{-1}. Values for the hardness and elastic modulus were obtained from

* Corresponding author at: Università di Torino, NIS Centre of Excellence, Dipartimento di Chimica IFM, via P. Giuria 7, I-10125 Torino, Italy.
Tel.: +39 0116707140; fax: +39 0116707855.
E-mail address: alberto.castellero@unito.it (A. Castellero).

0925-8388/$ – see front matter © 2006 Elsevier B.V. All rights reserved.
doi:10.1016/j.jallcom.2006.08.168

the loading and unloading curves, respectively, according to the analysis method reported in Ref. [11]. Transmission electron microscopy was performed on a Philips CM30 TEM at 300 kV. Samples for TEM observations were thinned along the cross-section of the indents in an FEI FIB200 workstation (see Ref. [12] for details). A protective Au layer was sputtered on the sample surface before imaging in the FIB. A small strip of Pt was deposited over the indent in the FIB before milling was commenced. Air corrosion of the freshly indented $Mg_{66}Ni_{20}Nd_{14}$ was precluded by covering the surface with mounting wax.

3. Results

3.1. $Mg_{60}Cu_{30}Y_{10}$

The loading curves in Fig. 1 (loading rate of 1.0 mN s^{-1}) show the presence of constant-load steps, corresponding to the initiation and propagation of the shear bands, both in the case of the as-cast BMG (curve (a)), and of a partially crystallized sample after annealing at 185 °C for 11 min (curve (b)). The partially devitrified sample, containing orthorhombic Mg_2Cu crystals, shows a higher hardness ($H = 4.0 \pm 0.1$ GPa) and Young's modulus ($E = 60.0 \pm 0.5$ GPa) than the as-cast BMG ($H = 3.3 \pm 0.1$ GPa and $E = 51.5 \pm 1.5$ GPa). In the partially crystallized samples, the average crystal diameter, estimated from the broadening of the XRD peaks, is less than 70 nm.

Fig. 2(a) shows the intersection between one shear band and the sample surface, suggesting, in accordance with the nanoindentation curve, that the band propagation is not affected by the presence of the crystals. The Fresnel image at a defocus of +10 μm in Fig. 2(b) shows the presence of Mg_2Cu crystals, with diameter between 30 and 80 nm, together with regions (marked by arrows) where some of the density change associated with the shear bands did not relax completely, possibly due to the presence of the crystals. It can be ruled out that the crystallites visible below the indenter tip in Fig. 2(a) are stress-induced, since no crystals are observed under any indents other than the one in Fig. 2(a).

Fig. 3 shows a dark-field image, with the selected-area diffraction (SAD) from the first diffracting ring for the same indented region as that in Fig. 2(b). The contrast between the region beneath the indent, diffracting less strongly, and the undeformed surrounding volume suggests that local modification of the structure has occurred.

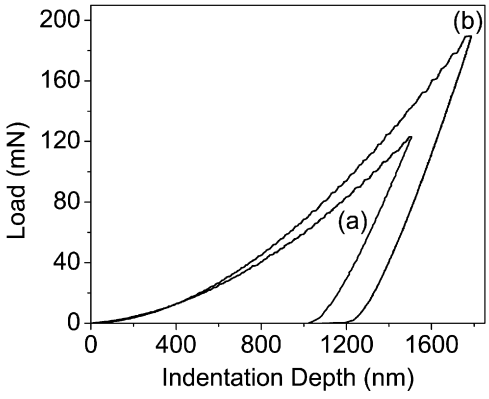

Fig. 1. Depth-sensing indentation loading and unloading curves for $Mg_{60}Cu_{30}Y_{10}$. Constant-load steps, associated with the nucleation and propagation of shear bands, are visible upon loading for both the as-cast BMG: curve (a) (maximum load 120 mN); and the partially crystallized glass: curve (b) (maximum load 190 mN).

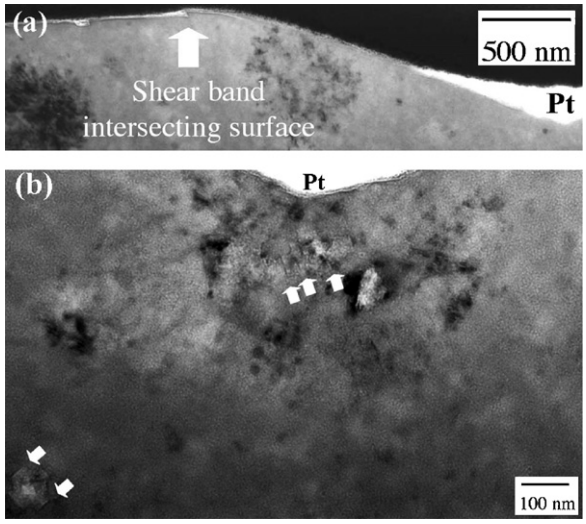

Fig. 2. (a) Bright-field image of an indent profile (penetration depth 900 nm) where a shear band intersects the surface of partially crystallized $Mg_{60}Cu_{30}Y_{10}$. (b) Fresnel image (defocus of +10 μm) of the region below an indent (penetration depth of 700 nm). The arrows indicate the presence of shear bands, which did not relax completely.

3.2. $Mg_{66}Ni_{20}Nd_{14}$

The loading curves of Fig. 4 show that the constant-load steps observed in the as-cast BMG (curve (a)) disappear after partial crystallization (curve (b)). The precipitation of hexagonal Mg_2Ni crystals in the remaining amorphous matrix leads to values of hardness ($H = 4.3 \pm 0.1$ GPa) and Young's modulus ($E = 72 \pm 2$ GPa) higher than those for the fully amorphous sample ($H = 3.4 \pm 0.2$ GPa and $E = 57 \pm 1$ GPa) at a load of 300 mN.

The bright-field image of Fig. 5(a), related to the cross-section of an indent with a depth of 400 nm in partially devitrified $Mg_{66}Ni_{20}Nd_{14}$, shows no evidence of shear bands intersecting the sample surface, but exhibits a low-density region, full of voids, just below the tip of the indent. The size of this region

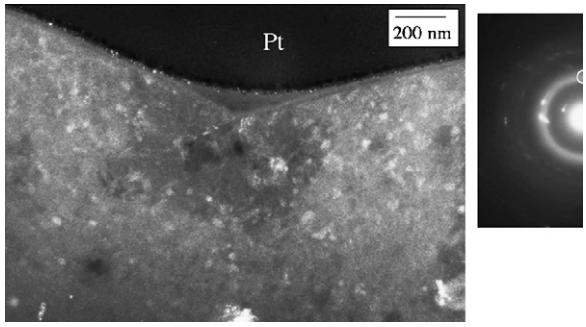

Fig. 3. Partially crystallized $Mg_{60}Cu_{30}Y_{10}$: dark-field image (SAD on the first diffracting ring) of the same indent profile as the one in Fig. 2(b). A contrast between the region beneath the indent, diffracting less strongly, and the undeformed surrounding volume is visible.

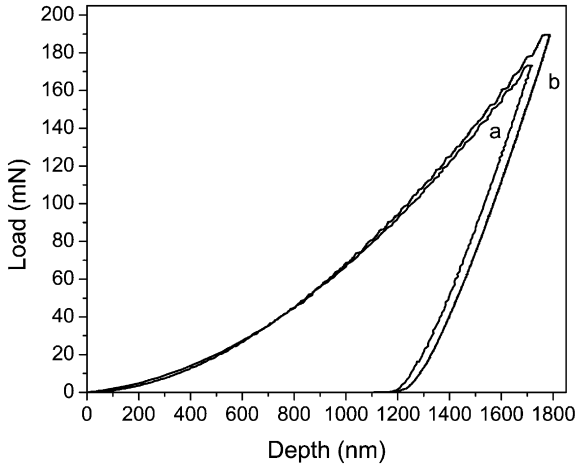

Fig. 4. Loading and unloading curves for $Mg_{66}Ni_{20}Nd_{14}$. The constant-load steps, present in the loading curve of the as-cast BMG (a), disappear in the partially crystallized sample (b).

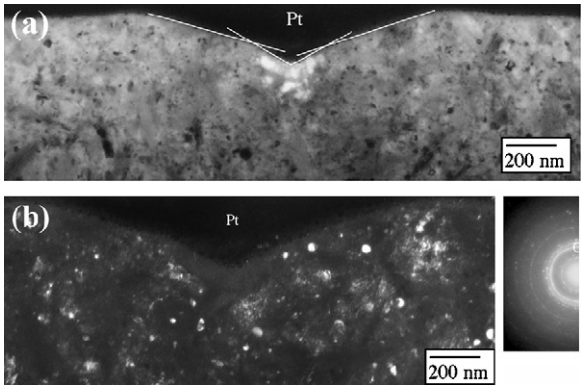

Fig. 5. Indent cross-section (penetration depth 400 nm) in partially devitrified $Mg_{66}Ni_{20}Nd_{14}$. (a) Bright-field image. Corresponding to a porous region surrounding the tip, the indent profile becomes steeper suggesting that the material did not recover elastically after deformation. (b) Dark-field image with aperture on the second diffracting ring. Equiaxed (30–40 nm diameter) and elongated crystals (70 nm × 250 nm), both corresponding to hexagonal Mg_2Ni, are visible.

does not seem to be dependent on the indentation depth or the applied load, since the same extent (∼150–200 nm) is observed under indents with depths ranging from 200 to 1700 nm. The white lines show that the indent profile becomes steeper corresponding to the low-density region, as if the material had not recovered completely after the deformation. Such features are not observed in the as-cast BMG.

The crystallized volume, comprising equiaxed (30–40 nm diameter) and elongated crystals (∼70 nm × 250 nm), is estimated at around 50%. The average crystal diameter deduced from the broadening of the XRD peaks is about 200 nm. The diffraction rings of Fig. 5(b) confirm that the crystals match the hexagonal structure of Mg_2Ni ($a = 0.5198$ nm, $i = 1.321$ nm).

4. Discussion

The presence of the constant-load steps in the loading curves of $Mg_{60}Cu_{30}Y_{10}$ for different crystallized fractions was explained by suggesting that, for low-crystallized fraction, the crystals are not large enough to inhibit shear-band propagation and, for a higher crystallized fraction, that the plastic deformation partially occurs in the crystals through conventional dislocation glide [10].

The change in contrast between the region below the indent and the undeformed surrounding area, shown in Fig. 3, can be explained by a local structural modification such as the formation of short/medium-range order in the zone undergoing deformation. Similar features were observed after relaxation upon annealing, when the free volume annihilation in the glass leads to a topological (or chemical) short-range ordering of the atoms (see Ref. [13] and references therein).

In the case of partially crystallized $Mg_{66}Ni_{20}Nd_{14}$, the most interesting results are the low-density region and the non-linear profile of the indent cross-section. Concerning the presence of these two features, the possible presence of an artefact due to the removal of some material during the FIB procedure was taken into account. First of all it should be acknowledged that FIB is one of the most suitable techniques for thinning brittle, highly stressed and inhomogeneous materials [14,15], and probably the only one for cross-sectioning such small indents. If the voids had been induced by FIB thinning they should be visible across the whole sample rather than being localized in the indented region. In our case, the region immediately below the indent was highly stressed after withdrawing the indenter, since the material was not able to recover elastically upon unloading. It might be thought that the voids were caused by the removal of the brittle intermetallic Mg_2Ni during ion irradiation of this stressed region. Even if this were the case, the presence of the voids would still be related to a real feature of the material. In fact, the hypothetical removal of the crystals would have occurred in selected regions, with different properties (i.e. higher stress concentration) than the surrounding material. The non-constant profile of the indent cross-section was also unlikely to be caused by preferential milling, since the layer of gold, deposited on the surface of the indents prior to any ion irradiation, was still uniform after FIB thinning.

The formation of the void region can be explained by free volume coalescence [4] due to the collapse of the shear bands, this originating from the indenter tip, which cannot propagate because of the presence of crystals with diameter larger than the shear-band thickness. Consequently, the material around the indent cannot recover elastically, causing a change in the slope of the indent profile.

5. Conclusions

In this work, nanoindentation, FIB and TEM techniques were combined in order to study the effect of different crystal sizes and crystal distributions on the propagation of shear bands from the indenter tip through the remaining amorphous matrix in $Mg_{60}Cu_{30}Y_{10}$ and $Mg_{66}Ni_{20}Nd_{14}$.

In $Mg_{60}Cu_{30}Y_{10}$, the propagation of shear bands is not affected by the presence of crystals with diameters comparable to the shear-band thickness. The increase in

density of the amorphous material below the indent tip can be explained by the formation of short/medium-range order.

In $Mg_{66}Ni_{20}Nd_{14}$, shear-band activity is clearly disturbed by crystals with diameter one order of magnitude larger than the shear-band thickness. We propose that the low-density region under the indent and the slope change of the indent profile are due to the coalescence of the free volume contained in the shear bands stopped by the crystals.

Acknowledgements

This work was supported financially by the Royal Society of London, ETH Research Grant TH-21/04-2, the Postdoctoral Research Program (D048461) of the Hungarian Scientific Research Grant and Ductilisation of Bulk Metallic Glasses (BMGs) by Length-scale Control in BMG Composites and Applications (Contract MRTN-CT-2003-504692).

References

[1] C.A. Pampillo, J. Mater. Sci. 10 (1975) 1194.
[2] F. Spaepen, Acta Metall. 25 (1977) 407.
[3] P.E. Donovan, W.M. Stobbs, Acta Metall. 29 (1981) 1419.
[4] J. Li, F. Spaepen, T.C. Hufnagel, Philos. Mag. A82 (2002) 2623.
[5] Y.I. Golovin, V.I. Ivolgin, V.A. Khonik, K. Kitagawa, A.I. Tyurin, Scripta Mater. 45 (2001) 947.
[6] W.J. Wright, R. Saha, W.D. Nix, Mater. Trans. 42 (2001) 642.
[7] A.L. Greer, I.T. Walker, Mater. Sci. Forum 386–388 (2002) 77.
[8] C.A. Schuh, T.G. Nieh, Y. Kawamura, J. Mater. Res. 17 (2002) 1651.
[9] A.L. Greer, A. Castellero, S.V. Madge, I.T. Walker, J.R. Wilde, Mater. Sci. Eng. A 375–377 (2004) 1182.
[10] Zs. Kovács, A. Castellero, A.L. Greer, J. Lendvai, M. Baricco, Mater. Sci. Eng. A 387–389 (2004) 1012.
[11] W.C. Oliver, G.M. Pharr, J. Mater. Res. 7 (1992) 1564.
[12] S.J. Lloyd, J.M. Molina-Aldareguia, W.J. Clegg, Philos. Mag. 82 (2002) 1963.
[13] C.A. Schuh, T.G. Nieh, J. Mater. Res. 19 (2004) 46.
[14] M. Sugiyama, G. Sigesato, J. Electron Microsc. 53 (2004) 527.
[15] C.A. Volkert, B. Heiland, F. Kauffmann, Prakt. Metallogr. 40 (2003) 193.